Physics of the Solid State, 2023, Vol. 65, No. 10

13,03

Synchrotron radiation effect on the AlN thermal conductivity

© *D.A. Chernodoubov*[1], *E.N. Mokhov*[2], *S.S. Nagalyuk*[2], *A.V. Inyushkin*[1]

[1] National Research Center „Kurchatov Institute“,
Moscow, Russia
[2] Ioffe Institute,
St. Petersburg, Russia
E-mail: Chernodubov_DA@nrcki.ru

Received July 19, 2023
Revised August 10, 2023
Accepted August 15, 2023

The effect of synchrotron radiation on the thermal conductivity of an AlN single crystal was studied in the temperature range from 5 to 410 K. It was found that in the intermediate temperatures region (20−70 K) the thermal conductivity of irradiated sample decreases by 11%, while in the region of high temperatures above 150 K the effect is negligible. Within the framework of the first-principles approach, the temperature dependence of the thermal conductivity of an AlN crystal with a wurtzite-type structure was calculated. The calculation results are in a satisfactory agreement with the experimental data at temperatures above 200 K. It is shown that the reason for such a change in the thermal conductivity and the nature of its temperature dependence may be the interaction of thermal phonons with the charge carriers bound to alloying defects in the crystal lattice (primarily with oxygen atoms and aluminum vacancies impurity complexes).

Keywords: single crystal, thermal conductivity, aluminum nitride, synchrotron radiation, first-principles calculations.

DOI: 10.61011/PSS.2023.10.57233.159

1. Introduction

Aluminum nitride AlN has good prospects in modern electronics, since its large band gap of 6.2 eV makes it possible to manufacture highly efficient light emitting diode (LED) devices in the deep ultraviolet spectrum based on it, and it can be used as a substrate for the epitaxial growth of thin films of other semiconductor materials due to close values of lattice constants [1]. Using AlN single crystals and thin films, it is possible to produce a large number of microelectromechanical systems, such as energy storage devices, volumetric film acoustic resonant cavities, sensors, detectors, microphones, and chip-size communication converters [2]. Besides, the possibility of producing AlN-based memristors with long state retention times [3], high switching speeds, and energy efficiency has [4] was recently shown, which allows them to be considered for use in neuromorphic calculations [5–7].

One of the key properties of AlN is its high thermal conductivity, reaching $316\,\mathrm{W/(m\cdot K)}$ at room temperature in the case of a bulk single crystal [8]. As in other wide-band semiconductors, the phonons is the main heat carrier in AlN, and the electrons contribution to heat transfer is negligible practically over the entire temperature range. The main processes of phonon scattering that affect the thermal conductivity of the crystal are anharmonic processes of phonon-phonon scattering (normal and with quasi-momentum transfer), scattering at the crystal boundary, and on defects, both extended (such as dislocations) and point ones, including on the isotopes of the chemical elements that make up the compound. The latter is negligible in the case of AlN, since aluminum is monoisotopic, and in the natural composition of nitrogen isotopes the content of isotope ^{14}N is 99.636% and only 0.364% of ^{15}N.

The main point defects in AlN crystals are impurity atoms of O, C, Si and aluminum vacancies. From ab initio calculation it was found that of the above defects the aluminum vacancies have the greatest influence on the amount of heat transfer at relatively high temperatures due to the largest mass defect they introduce [9]. Thus, the presence of aluminum vacancies in the crystal at a concentration of $4\cdot 10^{18}\,\mathrm{cm^{-3}}$ leads to decrease in thermal conductivity by almost 10% at 300 K. A similar decrease in thermal conductivity relative to the pure sample (about 12%) was experimentally shown for crystals with concentration of impurity oxygen atoms equal to $4.2\cdot 10^{19}\,\mathrm{cm^{-3}}$ [10]. Moreover, since oxygen is introduced into aluminum nitride together with the aluminum vacancy, it is believed that in the case of such impurities the presence of vacancies is the main reason for phonon scattering. Dislocations, as a rule, are not a significant factor for the thermal conductivity of wide-band semiconductor crystals as a whole. Thus, it was shown that in the case of GaN the dislocations begin to influence the thermal conductivity only at a very high density (above $10^{10}\,\mathrm{cm^{-2}}$) [11].

The above types of phonon scattering make the main contribution at high temperatures. In the low-temperature region the thermal conductivity of the almost ideal crystal shall be limited solely by scattering at the crystal boundary, corrected for the anisotropy of the elastic properties of the

crystal, leading to the appearance of thermal conductivity anisotropy (phonon focusing). In the case of AlN it can be expressed in a difference in thermal conductivity values by approximately 20% for directions in the basal plane and along the axis c [12]. At that, the value of thermal conductivity shall depend on temperature as T^3. Such dependence was not observed in any of the low-lemperature measurements performed for the bulk single-crystals AlN [8,13,14]. Experiments differ rather significantly from theoretical calculations — in the temperature dependence of thermal conductivity the asymmetric maximum appears, it is shifted to temperatures by almost two times exceeding the design temperature as its value decreases, and at low temperatures the exponential function of thermal conductivity is significantly weaker than the expected cubic one.

Recently, to explain the nature of the temperature dependence of the thermal conductivity of AlN the authors proposed a mechanism of scattering by charge carriers associated with impurity atoms [8]. The same scattering mechanism has a significant effect on heat transfer in the region of maximum thermal conductivity and below in the case of another wide-band semiconductor-diamond [15]. It is based on that low-frequency phonons interact not with the impurity itself, but with the charge carrier coupled with it by changing the energy of the impurity levels due to the deformation that occurs during the phonons propagation, that is, a virtual transition of carriers between impurity levels occurs. Accordingly, the magnitude of this scattering correlates not with the total concentration of impurities, but with the concentration of impurities charged in a certain way. The magnitude of such scattering can be by orders of magnitude greater than scattering by mass defect caused by point impurity. For low-frequency phonons with a wavelength exceeding the Bohr radius of the impurity center, it depends on the phonon frequency ω approximately as ω^4; this explains the suppression of thermal conductivity to the left of the maximum. On the other hand, for high-frequency phonons, when the threshold frequency is exceeded, when the phonon wavelength is compared with the size of the wave function of the bound carrier, the contribution of this scattering to heat transfer drops sharply, so it practically does not affect the value of thermal conductivity at sufficiently high temperatures to the right of the thermal conductivity maximum. As a result, scattering of phonons on carriers bound with doping impurities often leads to the asymmetry of the thermal conductivity peak — with thermal conductivity suppression at low temperatures. The detailed description of this scattering process and the expressions defining it is given in the article [15] and additional materials to it.

To study the scattering process on bound carriers, in this paper we irradiated the sample with synchrotron radiation — it is known that in the case of ceramic AlN the change in the charge state of defects associated with vacancies under the exposure to the ultraviolet radiation leads to decrease in thermal conductivity by 4% at temperature of 295 K [16]. In our case, irradiation led to the excitation of charge carriers bound with defects and change in the nature of the temperature dependence of thermal conductivity — in the temperature range of about 100 K and below, the thermal conductivity decreased by 11%, while in the range of high temperatures the effect turned out to be negligible.

2. Methods

For irradiation and measurements the same AlN2 sample was used as described in [8]. The initial AlN single crystal with wurtzite-type crystal lattice was grown by the PVT method in a tungsten crucible with a graphite heater. A specially prepared aluminum nitride crystal with (0001)Si orientation was used as a nucleus. Commercially available high purity AlN powder (ABCR GmbH (Germany), grade A) was used. The impurity content in the original powder was less than a few ppm. The powder was annealed in vacuum at a temperature of 1600°C for 10 h, and then in a nitrogen atmosphere at temperature of 2150°C for 30 h to reduce the concentration of impurities. The crystal was grown at a rate of about 50 μm/h at a temperature in the range 1900−2000°C in nitrogen atmosphere (N_2 purity 99.999% at pressure of 250 Torr). The crystal growth process is described in more detail in [17]. To measure thermal conductivity a parallelepiped-shaped sample with dimensions $6.6 \times 3.0 \times 0.63\,\mathrm{mm}^3$ was cut from the original crystal.

The temperature dependence of thermal conductivity was measured using the longitudinal heat flow method. The heat flow during the measurements was directed in the basal plane and, accordingly, the thermal conductivity value in the basal plane was measured. A detailed description of the experimental procedure is given in [18]. The experimental error of measurements does not exceed 3% in the main measurement range, but increases by several times near the boiling point of liquid helium, and at 400 K reaches 4%.

According to secondary ion mass spectrometry, the sample contains impurity atoms of carbon, oxygen and silicon in a concentration of $[\mathrm{C}] \approx 5 \cdot 10^{18}\,\mathrm{cm}^{-3}$, $[\mathrm{O}] \approx 6 \cdot 10^{18}\,\mathrm{cm}^{-3}$, $[\mathrm{Si}] \approx 5 \cdot 10^{17}\,\mathrm{cm}^{-3}$. The concentration of paramagnetic defects in the sample, according to SQUID magnetometry data, lies in the range $(1-3) \cdot 10^{17}\,\mathrm{cm}^{-3}$. Measurements of the Raman spectrum confirmed that at room temperature the concentration of free charge carriers in them is negligible, and lattice deformation due to the presence of defects and impurities is insignificant.

The sample irradiation with synchrotron radiation was carried out at „Kurchatov SRSS“ („Large storage ring of Kurchatov synchrotron radiation special source“). Critical energy of synchrotron radiation — 7.1 eV, beam size — $5 \times 1\,\mathrm{mm}^2$. The sample was fixed at a distance of 16 m from the radiation source (output from a bending magnet) behind three beryllium foils 150 μm thick each, which made it possible to cut off the soft part of the spectrum with energies below 3 keV. Photographs of the sample before and

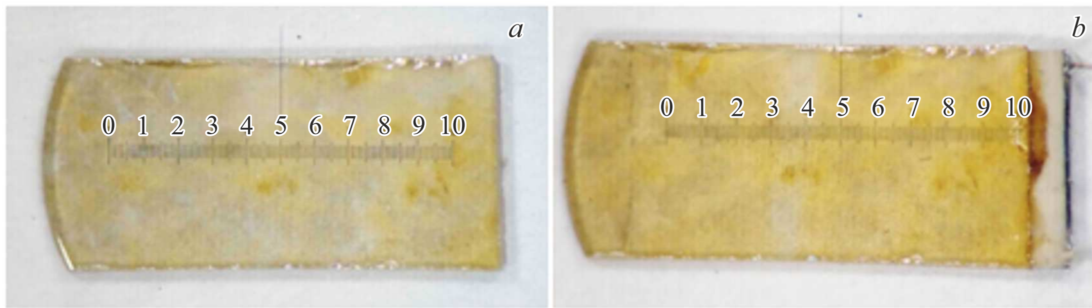

Figure 1. AlN2 sample before and after irradiation.

after irradiation are shown in Figure 1. It can be seen that the crystal color changed from pale yellow to bright yellow. The initial pale yellow color of the crystal may be caused by nitrogen vacancies in the paramagnetic neutrally charged state [19]. Presumably, irradiation affected the energy state of the defects present in the crystal. As the sample was mounted, the brightness of its color decreased, which we associate with the reversibility of changes in charge state of defects under the influence of visible light. It took about 1h from the moment of irradiation until the sample was cooled to cryogenic temperatures.

To ab initio calculate the thermal conductivity the ShengBTE program [20] was used. Under this approach the thermal conductivity of the crystal is defined as:

$$\kappa_{\alpha\beta} = \sum_{\lambda} C_{\lambda} \nu_{\lambda,\alpha} \vartheta_{\lambda,\beta} \tau_{\lambda,\beta}, \qquad (1)$$

where summation is performed over all phonon modes $\lambda \equiv (\mathbf{q}, j)$ with wave vector $\mathbf{q}$ and polarization j; C_{λ} — specific (volume) heat capacity of phonon mode λ; $\nu_{\lambda,\alpha}$ — group velocity of mode λ along direction α in rectangular (Cartesian) coordinate system, τ_{λ} — mode lifetime λ. Phonon spectrum and phonon relaxation times in three-phonon scattering processes was calculated on grid $26 \times 26 \times 14$ of wave vectors in the Brillouin zone. For the calculation the second- and third-order force constants were used, calculated using the supercell $5 \times 5 \times 5$ from the data base of project AlmaBTE [22,23].

Further, the thermal conductivity values are determined by solving the Boltzmann transport equation taking into account three-phonon scattering processes, scattering by impurity isotopes and boundary scattering. The scattering velocity in all phonon processes are summed up in accordance with Matthiessen's rule. To calculate the contribution of boundary scattering, we used the Casimir path length calculated from the sample geometry, $l_C = 1.34$ mm.

3. Results and discussion

The result of measuring the temperature dependence of the thermal conductivity of AlN single crystal is shown in Figure 2; the sample after irradiation is designated as AlN2x. The qualitative shape of the curve corresponds to that typical for wide-band semiconductor materials — at high temperatures the thermal conductivity decreases due to the growing contribution of phonon-phonon scattering, and at low temperatures — due to the „freezing out" of high-frequency acoustic phonon modes while maintaining influence of scattering by the crystal surface. It can be seen that irradiation did not affect the value of thermal conductivity in the region of high temperatures above 150 K — the difference in the measured values of thermal conductivity of the sample before and after irradiation is within the experimental error and is below 2%. In this case, the value of the maximum of thermal conductivity as a result of irradiation decreased by about 4%, and the maximum itself shifted upward in temperature from 67.5 to 70.5 K. This change, together with the asymmetry of the maximum of thermal conductivity, indicates the increase in the additional process of phonon scattering in the low temperature region. Previously, the authors [8] proposed scattering by charge carriers bound with impurity donors/acceptors as such phonon scattering process in the case of AlN crystals. As can be seen from the experiment, the maximum effect of this scattering occurs at temperature of 35 K, as shown in the insert of Figure 2. This is consistent with previous papers on the study of the low-temperature dependence of the thermal conductivity of AlN: in [8], based on the Bohr radius of 15 Å of the donor in AlN the estimate of the temperature of the maximum influence of scattering by bound charge carriers was obtained at 22 K, and in the same range 20−30 K there is „dip" in the thermal conductivity of the oxygen heavily-doped AlN R162 [10] sample.

To further understand the nature of scattering by bound carriers, the ab initio calculation of the thermal conductivity of AlN single crystal was carried out, since defect-free AlN crystals on which it would be possible to measure thermal conductivity and experimentally determine the contribution of this scattering are currently unavailable. It is shown that the results of ab initio calculations agree very well with experimental measurements, and they can be used as „reference" for the almost ideal crystal [24]. The result of the calculation in comparison with the experimental

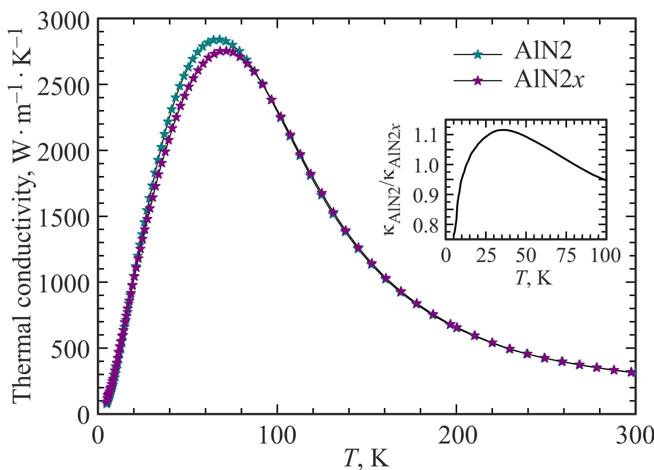

Figure 2. Thermal conductivity vs. temperature of aluminum nitride single crystal before (AlN2) and after (AlN2x) irradiation with synchrotron radiation. The insert shows the ratio of thermal conductivity values below 100 K.

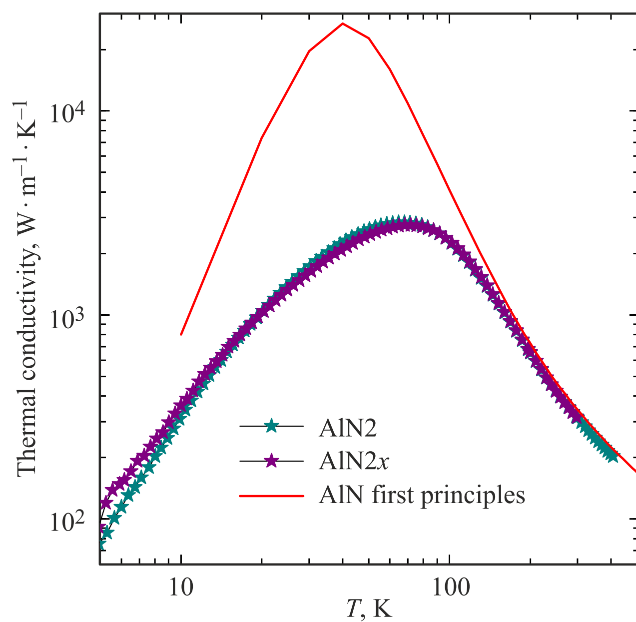

Figure 3. Thermal conductivity vs. temperature of AlN crystal. The solid red line shows the results of ab initio calculations, the dots show experimental data.

data is shown in Figure 3. At 300 K, the experimental value of thermal conductivity is 316 W/(m · K), and the calculated value is 343 W/(m · K). This difference, within 10%, is most likely due to the phonons scattering by point defects, which are in a rather high concentration for the crystal understudy. This is also supported by the fact that the slope of the thermal conductivity curve in the high-temperature region practically did not change relative to that calculated for the ideal crystal. The main difference between the curves is observed in the temperature range near the maximum of thermal conductivity — the value of thermal conductivity differs by an order of magnitude in experiment and calculation, although in calculations the geometry of the crystal was used on which the measurements were carried out, and, as a rule, at low temperatures boundary scattering plays a decisive role. It can be seen that the difference between the calculated thermal conductivity and the measured one in the initial state is similar to the difference in the temperature dependence of the thermal conductivity of the sample before and after irradiation, and just the maximum shifts down and to the right. The phonon focusing effect, not considered in the ab initio calculation, cannot explain such a significant difference between calculation and experiment at low temperatures, since its value for AlN in the direction of the basal plane does not exceed 8% [12]. This is caused by scattering by bound carriers. The original crystal contains various defects (donors and acceptors) in different charge states, some of them are positively charged, and some are negatively charged, while their total charge is zero. Irradiation changes the charge distribution between these centers, changing the content of charged and neutral centers, increasing the proportion of negatively charged defects. As a result, the dissipation efficiency at low temperatures could decrease, which led to increase in the thermal conductivity in the temperature range 5−20 K, but the dissipation efficiency increased near the maximum of thermal conductivity. A similar effect was previously observed in the case of single-crystal germanium doped with antimony and antimony with gallium (compensated) [25]. The effect of such a pair of dopant impurities on the temperature dependence of the thermal conductivity of Ge is similar to the observed effect of irradiation on the thermal conductivity of AlN. The sample, in which in addition to donors (antimony) there are also acceptors (gallium), has a higher thermal conductivity near the maximum, but is reduced in the temperature range below the maximum. Since the main defects in AlN are complexes of impurity oxygen with aluminum vacancies, we can conclude that change in the energy state of the charge carriers bounded with them led to the observed change in thermal conductivity, and scattering by these defects plays the decisive role in the temperature dependence of the thermal conductivity of AlN at temperatures near and below maximum thermal conductivity.

4. Conclusion

The temperature dependence of the thermal conductivity of AlN sample was measured before and after irradiation with synchrotron radiation in wide temperature range from 5 to 400 K. It is shown that as a result of change in the state of charge carriers bound with doping defects, the amount of thermal phonon scattering changes, which leads to significant change in the value and behavior of thermal conductivity in the region of maximum thermal conductivity, namely, the shift of the maximum of thermal conductivity towards high temperatures and to decrease in its value. In

the region of low temperatures the dependence of thermal conductivity deviates from cubic one, while in the region of high temperatures no changes are observed. Together with the ab initio calculation, these data show the role of phonon scattering by charge carriers bound with doping defects (presumably, in the case of AlN, such defect is a complex of impurity oxygen with aluminium vacancy). The data obtained make it possible to refine existing models of heat transfer in wide-band crystals and can be used to simulate the thermal behavior of AlN-based devices.

Acknowledgments

The authors are grateful to A.V. Rogachev (National Research Center „Kurchatov Institute") for assistance in conducting the experiment using synchrotron radiation and A.N. Taldenkov (National Research Center „Kurchatov Institute") for measuring the magnetization of the samples.

Funding

This study was funded by the Ministry of Science and Higher Education of the Russian Federation under Agreement No. 075-15-2021-1357 using the equipment of UNU „KISS". E.N. Mokhov and S.S. Nagalyuk thank the Ioffe Physico-Technical Institute of the Russian Academy of Sciences for their support.

Conflict of interest

The authors declare that they have no conflict of interest.

References

[1] R. Yu, G. Liu, G. Wang, C. Chen, M. Xu, H. Zhou, T. Wang, J. Yu, G. Zhao, L. Zhang. J. Mater. Chem. C **9**, 1852 (2021).
[2] R.M. Pinto, V. Gund, R.A. Dias, K. Nagaraja, K. Vinayakumar. J. Microelectromechanical Sys. **31**, 500 (2022).
[3] Y. Guo, W. Hu, C. Zhang, Y. Peng, Y. Guo. J. Phys. D **53**, 195101 (2020).
[4] B.J. Choi, A.C. Torrezan, J.P. Strachan, P. Kotula, A. Lohn, M.J. Marinella, Z. Li, R.S. Williams, J.J. Yang. Adv. Funct. Mater. **26**, 5290 (2016).
[5] A.A. Minnekhanov, B.S. Shvetsov, A.V. Emelyanov, K.Y. Chernoglazov, E.V. Kukueva, A.A. Nesmelov, Y.V. Grishchenko, M.L. Zanaveskin, V.V. Rylkov, V.A. Demin. J. Phys. D **54**, 484002 (2021).
[6] B.S. Shvetsov, A.V. Emelyanov, A.A. Minnekhanov, K.E. Nikiruy, A.A. Nesmelov, M.N. Martyshov, V.V. Rylkov, V.A. Demin. Ros. nanotekhnologii **14**, 85 (2019). (in Russian)
[7] K.E. Nikiruy, A.V. Emelyanov, V.A. Demin, A.V. Sitnikov, A.A. Minnekhanov, V.V. Rylkov, P.K. Kashkarov, M.V. Kovalchuk. AIP Adv. **9**, 065116 (2019).
[8] A.V. Inyushkin, A.N. Taldenkov, D.A. Chernodubov, E.N. Mokhov, S.S. Nagalyuk, V.G. Ralchenko, A.A. Khomich. J. Appl. Phys. **127**, 205109 (2020).
[9] R.L. Xu, M. Munoz Rojo, S. Islam, A. Sood, B. Vareskic, A. Katre, N. Mingo, K.E. Goodson, H.G. Xing, D. Jena, E. Pop. J. Appl. Phys. **126**, 185105 (2019).
[10] G.A. Slack, R.A. Tanzilli, R. Pohl, J. Vandersande. J. Phys. Chem. Solids **48**, 641 (1987).
[11] J. Zou, D. Kotchetkov, A.A. Balandin, D.I. Florescu, F.H. Pollak. J. Appl. Phys. **92**, 2534 (2002).
[12] D.A. Chernodoubov, A.V. Inyushkin. Phys. Lett. A **384**, 126120 (2020).
[13] G.A. Slack, L.J. Schowalter, D. Morelli, J.A. Freitas Jr. J. Cryst. Growth **246**, 287 (2002).
[14] R. Rounds, B. Sarkar, A. Klump, C. Hartmann, T. Nagashima, R. Kirste, A. Franke, M. Bickermann, Y. Kumagai, Z. Sitar, R. Collazo. Appl. Phys. Express **11**, 071001 (2018).
[15] A.V. Inyushkin, A.N. Taldenkov, V.G. Ralchenko, G. Shu, B. Dai, A.P. Bolshakov, A.A. Khomich, E.E. Ashkinazi, K.N. Boldyrev, A.V. Khomich, J. Han, V.I. Konov, J. Zhu. J. Appl. Phys. **133**, 025102 (2023).
[16] J.H. Harris, R.C. Enck, R.A. Youngman. Phys. Rev. B **47**, 5428 (1993).
[17] E.N. Mokhov, A.A. Wolfson. In: Single Crystals of Electronic Materials. Woodhead Publishing Series in Electronic and Optical Materials / Ed. R. Fornari. Woodhead Publishing (2019). Ch. 12. P. 401.
[18] A.V. Inyushkin, A.N. Taldenkov, V.G. Ralchenko, A.P. Bolshakov, A.V. Koliadin, A.N. Katrusha. Phys. Rev. B **97**, 144305 (2018).
[19] V.A. Soltamov, I.V. Ilyin, A.A. Soltamova, D.O. Tolmachev, N.G. Romanov, A.S. Gurin, V.A. Khramtsov, E.N. Mokhov, Y.N. Makarov, G.V. Mamin, S.B. Orlinskii, P.G. Baranov. Appl. Magn. Res. **44**, 1139 (2013).
[20] W. Li, J. Carrete, N.A. Katcho, N. Mingo. Comput. Phys. Commun. **185**, 1747 (2014).
[21] N.K. Ravichandran, D. Broido. Phys. Rev. B **98**, 085205 (2018).
[22] J. Carrete, B. Vermeersch, A. Katre, A. van Roekeghem, T. Wang, G.K.H. Madsen, N. Mingo. Comput. Phys. Commun. **220**, 351 (2017).
[23] https://almabte.bitbucket.io/database/
[24] L. Lindsay, C. Hua, X.L. Ruan, S. Lee. Mater. Today Phys. **7**, 106 (2018).
[25] J.F. Goff, N. Pearlman. Phys. Rev. **140** (6A), A2151 (1965).

Translated by I.Mazurov